Molecular Relaxations in Ester-Terminated, Amide-Based Dendrimers

SHAYLA K. EMRAN,[1] GEORGE R. NEWKOME,[2] CLAUS D. WEIS,[2] JULIE P. HARMON[1]

[1] Department of Chemistry, University of South Florida, Tampa, Florida 33620

[2] Center for Molecular Design and Recognition, University of South Florida, Tampa, Florida 33620

Received 14 October 1998; revised 22 February 1999; accepted 1 March 1999

ABSTRACT: This study utilized Matrix Assisted Laser Desorption/Ionization Time-of-Flight Mass Spectrometry, Thermogravimetric Analysis, Differential Scanning Calorimetry, X-Ray Diffraction, and Dielectric Analysis to assess the viscoelastic and structural properties of three generations of *tert*-butyl and methyl ester, amide-based dendrimers. The effect of generation number and functionality on glass-transition temperatures and corresponding apparent activation energies, obtained via adherence to WLF behavior, were determined. Both were found to increase with increasing generation number and bulkiness of terminal functionalities. WLF constants, C_1 and C_2, allowed the determination of free volume, and thermal expansion coefficients, respectively. Secondary transitions, conforming to Arrhenius behavior, were also characterized and increased in temperature with generation number. The apparent activation energy was greater when the matrix was crystalline. Dielectric relaxation responses were analyzed to yield dielectric strengths of the molecular relaxations which increased with generation number and were comparable for both *tert*-butyl and methyl esters in the glass-transition region. Electrical properties of the dendrimers were dominated by ionic conductivity in the high temperature region. In order to unmask the glass transition, the data were treated in terms of the electric modulus. © 1999 John Wiley & Sons, Inc. J Polym Sci B: Polym Phys 37: 2025–2038, 1999

Keywords: dendrimer; relaxations; dielectric analysis; electric modulus

INTRODUCTION

Synthesis of dendritic and hyperbranched structures has allowed the examination of novel macromolecular architectures. Newkome et al.[1] and Tomalia et al.[2] initially reported on dendrimers in 1985 and have written several reviews on this topic. While most available literature has focused on synthetic routes to these materials, physical characterization, is far from complete. Several investigations of glass-transition temperatures (T_g) in dendrimers[3–6] and hyperbranched structures[7–9] have correlated T_gs to the number of chain ends, number of monomer units, molecular weight, and chain end composition. Crystalline[4] and liquid-crystalline[5,10,11] states in these highly branched macromolecules have also been characterized; however, studies probing the viscoelastic nature of these structures (translational, segmental, and side-chain mobility) are sparse. Mourey et al.[12] studied poly (benzyl ether) dendrimers via differential viscosity coupled with size exclusion chromatography. They determined that for the 0 through 6th generations, the intrinsic viscosities of these cascades pass through a maximum in the third generation, whereas the refractive index passes through a minimum around the second

Correspondence to: J. P. Harmon (E-mail: harmon@chuma1.cas.usf.edu)

Journal of Polymer Science: Part B: Polymer Physics, Vol. 37, 2025–2038 (1999)
 CCC 0887-6266/99/162025-14

generation. This indicates a monotonic decrease in density from the periphery, as theoretically determined by DeGennes and Hervert.[13] Hawker et al.[14] examined a cascade family generated from 3,5-dihydroxybenzyl alcohol in which the melt viscosity profiles showed no critical entanglement molecular weight for molecules as high as 85,000 amu suggesting "ball-bearing-like" behavior. Voit[3] verified this unusual behavior in several hyperbranched aromatic and aliphatic polyesters. "Ball bearing" behavior led researchers to examine the use of these structures as rheology modifiers in blends. Kim and Webster[15] blended polystyrene with two different hyperbranched, brominated polyphenylene structures and then noted that upon their addition, the melt viscosity of polystyrene was reduced. The tensile modulus of a 2% blend was shown to increase while the flexural modulus remained unchanged when compared to pure polystyrene. Aryl–aryl interactions between the styrene and the polyphenylene structures were thought to increase the moduli. Massa et al.[16] reported that a blend of linear bisphenol A polycarbonate, PC, with an all-aromatic, hyperbranched polyester resulted in increased tensile and compression moduli as well as decreased strain to break when compared to that of pure PC.

The above melt viscosity studies revealed that dendrimers and hyperbranched structures do not exhibit a rubbery plateau; however, these studies cannot extend below the glass-transition temperature due to the nature of the test. Dynamic mechanical studies, using solid samples such as flex specimens, are not possible on pure dendrimers and hyperbranched structures because most cannot be molded into solid parts. The most useful method for studying the entire range of molecular motion from far below to far above T_g (and T_m for crystalline structures) is dielectric spectroscopy. To date, the literature reports only one study using dielectric properties of hyperbranched polyesters.[17–19] These authors identified glass transitions, which were characterized by Williams–Landel–Ferry behavior and secondary relaxations conforming to Arrhenius behavior. In their most recent study,[19] they report on the effect of end groups on glass and secondary transitions and compare results to those obtained for linear analogues. In their studies, hyperbranched molecules were blended with polyethylene since the hyperbranched structures did not form films.

Herein, we focus on the physical characterization of a specific class of ester- terminated, amide-based dendrimers. In the following work, matrix-assisted laser desorption/ionization time-of-flight mass spectrometry (MALDI-TOF MS) was used to determine molecular weight and X-ray diffractometry was employed for structure analysis. Thermogravimetric analysis aided in the assessment of thermal stability, while differential scanning calorimetry was utilized in the analysis of molecular relaxations, namely, glass transitions. These primary (α) as well as secondary (β and γ) relaxations were further characterized via dielectric analysis. In addition, conductivity effects were investigated. Our method of dielectric experimentation circumvents the need to blend powder dendrimers with a polymer matrix to produce a film. To our knowledge, this is the first work to conduct dielectric analysis on neat dendrimers.

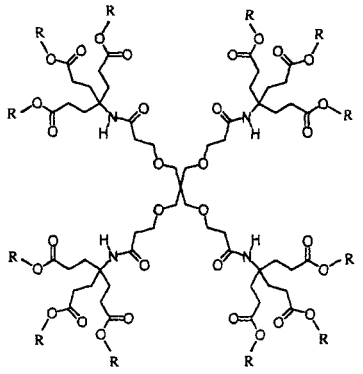

R = -C(CH$_3$)$_3$ **a**; -CH$_3$ **b**

C[CH$_2$OCH$_2$CH$_2$CONHC(CH$_2$CH$_2$CO$_2$R)$_3$]$_4$
Tier 1

C[CH$_2$OCH$_2$CH$_2$CONHC(CH$_2$CH$_2$CONHC(CH$_2$CH$_2$CO$_2$R)$_3$)$_3$]$_4$
Tier 2

C[CH$_2$OCH$_2$CH$_2$CONHC(CH$_2$CH$_2$CONHC(CH$_2$CH$_2$CONHC(CH$_2$CH$_2$CO$_2$R)$_3$)$_3$)$_3$]$_4$
Tier 3

Figure 1. Molecular structure and formula of 12-ester-terminated dendrimer (**1**), molecular formulas for 36- (**2**), and 108- (**3**) ester-terminated dendrimers.

EXPERIMENTAL

Materials

The *tert*-butyl dendritic samples were previously characterized and reported.[20] Figure 1 depicts the molecular structure of the first generation, or tier, where R represents either a *tert*-butyl or methyl terminal group, of which there are 12. The second and third tiers theoretically contain 36 and 108

termini, respectively. Figure 1 gives the molecular formulas for 12- (**1a**), 36- (**2a**), and 108- (**3a**) *tert*-butyl esters and 12- (**1b**), 36- (**2b**), and 108- (**3b**) methyl esters.

METHODS

Matrix-Assisted Laser Desorption/Ionization Time-of-Flight Mass Spectrometry

A Bruker II MALDI-TOF MS was utilized in the analysis of molecular weights. Insulin and cytochrome C were used as the standards for external calibration. A 10 mg/mL solution of the matrix, *trans*-3-indoleacrylic acid, was prepared in tetrahydrofuran (THF). Each sample ($\sim$ 1 mg) was first dissolved in 1.0 mL of THF, after which aliquots of 2.0 μL were added to 18 μL of the matrix solution. One drop of each final solution was placed on a numbered cell on the sample target. After evaporation, a thin film of the sample and matrix remained. Experimentation was conducted in the linear mode using *Xterm* and *Xacq* software for data acquisition.

Thermogravimetric Analysis*

Thermogravimetric Analysis (TGA) was conducted on a TA Instrument Hi Resolution TGA 2950. After the initial taring of empty platinum TGA pans, samples (2–6 mg) were placed on the pans and heated from 25°C to 500°C at a rate of 10°C/min under nitrogen. Flow rates to the furnace (sample) were between 34.0 and 38.0 mL/min, while flow rates to the balance ranged from 22.5 to 25.5 mL/min. The amount and rate of change in the weight of each sample were recorded as a function of temperature to determine thermal stability; a sensitivity of 0.1 μg and a balance accuracy of $\pm$0.1% were realized.[21]

Differential Scanning Calorimetry*

Differential Scanning Calorimetry (DSC) experiments were performed on a TA Instrument DSC 2920. Samples (5–10 mg) were hermetically sealed in aluminum DSC pans, as were empty reference pans. Under a 25 mL/min helium purge, samples and references were sequentially heated, cooled,** and reheated at a rate of 3°C/min from 0 to 150°C. The differential heat flow between the sample and reference was measured vs. temperature. The thermal history of the samples was erased upon the first heating; therefore, glass-transition temperatures were obtained from the second heating and were taken as the inflection point of the curve. Cooling and reheating of the samples allowed the assessment of potential recrystallization from the melt in the crystalline tiers. The DSC has a sensitivity of 0.2 μW, calorimetric precision of 1%, temperature reproducibility of 0.05°C, and temperature accuracy of $\pm$0.1°C.[22]

X-Ray Diffraction

Powder diffraction data for crystalline dendrimers were obtained with a Scintag XDS-2000 X-ray diffractometer utilizing Scintag DMS software and a wavelength of 1.54 Å.

Dielectric Analysis*

Dielectric Analysis (DEA) was conducted on a TA Instrument DEA 2970. In order to obtain dielectric spectra from the neat powder dendrimers, DEA ceramic single-surface sensors, equipped with a series of channels (125 μm wide and 12.5 μm deep) surrounded by electrodes, were utilized. After sensor calibration under a nitrogen purge of ca. 500 mL/min, the sample was distributed over the surface of the sensor, which rests on a furnace. When lowered, the ram applied a maximum force of 250 N to achieve a minimum spacing of 2.500 mm, thus embedding the powder into the channels. Spring-loaded electrical probes, protruding from the ram, made contact with electrical contact pads on the sensor to form the circuit. When voltage was applied, the sample response was measured as a function of temperature and frequency (0.1 and 100,000 Hz). Samples were run twice at a heating rate of 3°C/min from $-$150°C** to 150°C. The second scan was more reliable since, having passed through the glass transition during the initial heating, the sample achieved flow and uniformly distributed itself between the channels in the sensor. Cole–Cole data were subsequently obtained by heating the sam-

* A TA Instruments Thermal Analyst 2000 computer system equipped with data analysis software interfaced with TGA, DSC, and DEA.

** Programmed cooling in DSC experiments, as well as cooling to sub-ambient temperatures reaching $-$150°C in DEA experiments, was achieved with a TA Instruments Liquid Nitrogen Cooling Accessory (LNCA).

Table I. MALDI-TOF MS Data

	M_w	M_n	PD	Theoretical Molecular Weights (g/mol)
1a	2,046	2,046	1.00	2,015
2a	5,371	5,308	1.01	6,112
3a	13,784	13,620	1.01	18,404
1b	1,585	1,584	1.00	1,510
2b	4,559	4,457	1.02	4,597
3b	10,062	9,808	1.03	13,859

ples in 5°C increments within the given temperature range with 6-min isothermal measurements at each increment. The isothermal measurements allowed data acquisition over the entire frequency range. Capacitance and conductance were measured as a function of temperature and frequency to give the dielectric constant or permittivity, ε' (proportional to capacitance) and the loss factor, ε'' (proportional to conductance). The DEA offers a dielectric constant sensitivity of 0.01 and an isothermal stability of 0.2°C.[23]

RESULTS AND DISCUSSION

MALDI-TOF MS

Weight average and number average molecular weights (M_w and M_n) obtained via MALDI-TOF MS are given in Table I; the polydispersity (PD) and theoretical molecular weights are also listed. While first generation molecular weights closely coincide with theoretical values, defects are noted in the second- and third-generation molecular weights due to incomplete addition of the outer tier. It should be noted that the measured masses include associated cations, Na^+ and K^+ being the most common; this is more evident in the first generations.

TGA

TGA analysis revealed that the methyl esters (**1b**, **2b**, and **3b**) are thermally stable at temperatures up to 290°C. At approximately 235°C (Fig. 2), *tert*-butyl esters **1a** and **2a** lost 37.9% and 36.0% of their weights, respectively, which closely correspond to the theoretical amounts of isobutylene which would be produced due to the loss of the *tert*-butyl groups. It is well known that *tert*-butyl

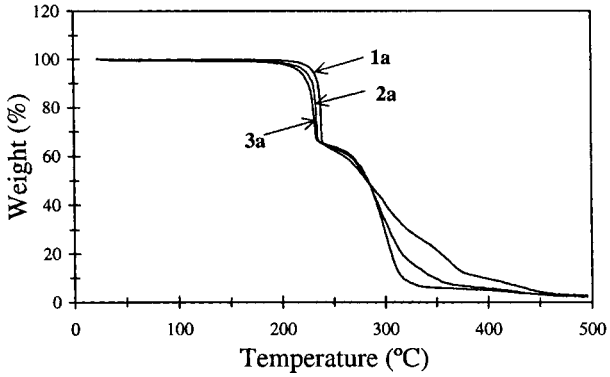

Figure 2. TGA plots for 12- (**1a**), 36- (**2a**), and 108- (**3a**) *tert*-butyl esters.

esters thermally eliminate isobutylene to generate the corresponding carboxylic acids, referenced in Table II as **1′**, **2′**, and **3′**. Dendrimer **3a** experienced a 34.2% weight loss from which it was determined that approximately only 84 of the 108 *tert*-butyl groups were present. Decomposition temperatures (T_d) of the carboxylic acid and methyl ester terminated structures are listed in Table II. Miller et al.[24] found that a fourth generation aryl ester dendrimer based on 1,3,5-benzenetricarboxylic acid was thermally stable up to 500°C at a heating rate of 10°C/min under N_2. However, the T_g (141°C) was much greater than those encountered for the dendrimers in this study. The elevated T_g indicates that degradation reactions are impeded by a lack of molecular mobility until much higher temperatures are reached.

DSC

Glass-transition temperatures and melting points were obtained via DSC and are listed in Table III. The glass-transition temperature was taken as the inflection point of the transition. The inflection point is the midpoint between the onset and offset of this relaxation. Only the first generations (**1a** and **1b**) were crystalline; the higher generations did not pack efficiently enough to form crys-

Table II. TGA Data (°C)

Loss of Isobutylene		T_d		T_d	
1a	238.5	**1′**	294.9	**1b**	293.0
2a	234.1	**2′**	295.4	**2b**	317.5
3a	231.6	**3′**	299.0	**3b**	310.7

Table III. DSC Relaxation Temperatures (°C) [Heating Rate 3°C/min]

	1a	2a	3a	1b	2b	3b
T_g	38	48	60	2	22	32
T_m	106			121		
T_c				97		

talline structures. Figure 3 depicts the DSC profile of the *tert*-butyl terminated, dendrimer **1a** for the first (A) and second (B) heating at a rate of 3°C/min to 150°C, well below its thermal expulsion of isobutylene. In the initial scan, two thermal transitions were observed, T_g and a melting endotherm, T_m, which appeared at 106.4°C (379.5. K). After controlled cooling at −3°C/min, subsequent heating revealed only a T_g at 38.3°C (311.4 K). The T_g/T_m ratio, 0.82, is typical for small molecules[9] (~ 0.75). The absence of T_m in the second scan was significant, as it revealed that crystallization of the neat dendrimer from the melt was unsuccessful; whereas, it readily crystallized from solution. Attempts to crystallize the dendrimer by annealing at temperatures between T_g and T_m were unsuccessful. The methyl-terminated dendrimer **1b** exhibited a melting transition in both the first and second scans. Figure 4 depicts the second scan and cooling curve which revealed a crystallization exotherm, T_c, signifying the recovery of crystallinity from the melt. As expected, subsequent heating resulted in the reappearance of a melting endotherm. T_g was observed in the second heating at 2.4°C (275.5 K) and the T_g/T_m ratio was 0.70. Analysis of dendrimers **2a**, **3a**, **2b**, and **3b** evidenced no melting endotherm and crystallization could not be induced from either solution or the melt. This corresponds well with data reported by Kim et al.[9] where it was determined that triphenylbenzene terminal functionality influenced the tendency of the structure to crystallize; derivatives possessing H, Br, and Cl end groups readily crystallized from the melt, while samples with OCH_3 and CH_2OCH_3 end groups only crystallized from solution.

In this study, it was shown that as the molecular weight increased with generation number, T_g also increased. Plots of T_g vs. molecular weight for linear polymers level off above a critical molecular weight. Similarly, glass-transition temperatures of dendrimers approach a constant value with increasing generation number; T_g values plateau around the fourth or fifth generation. It is uncertain where the T_g vs. molecular weight curve plateaus for the dendrimers in this study.

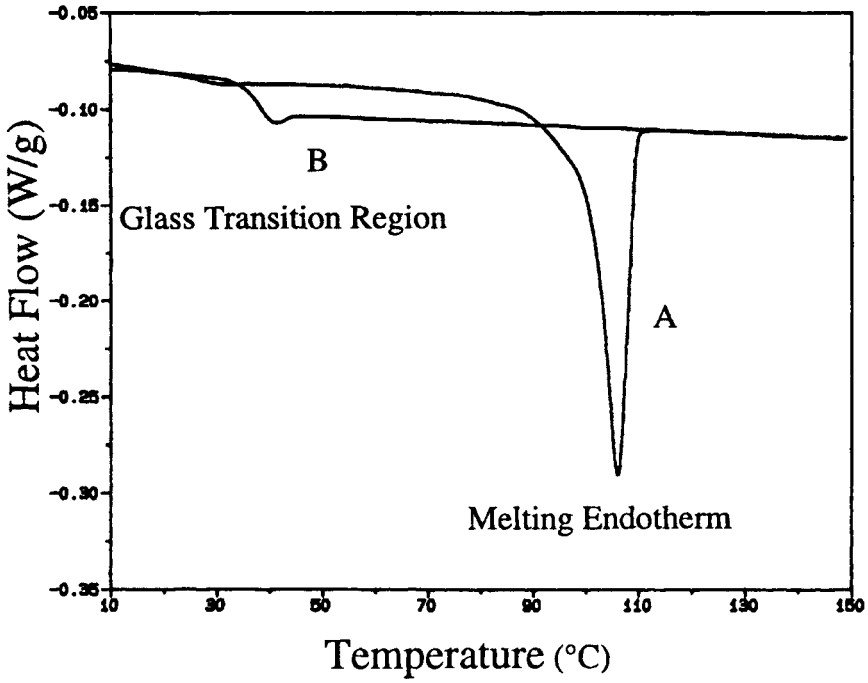

Figure 3. DSC plot for 12-*tert*-butyl ester (**1a**): (A) first heating; (B) second heating.

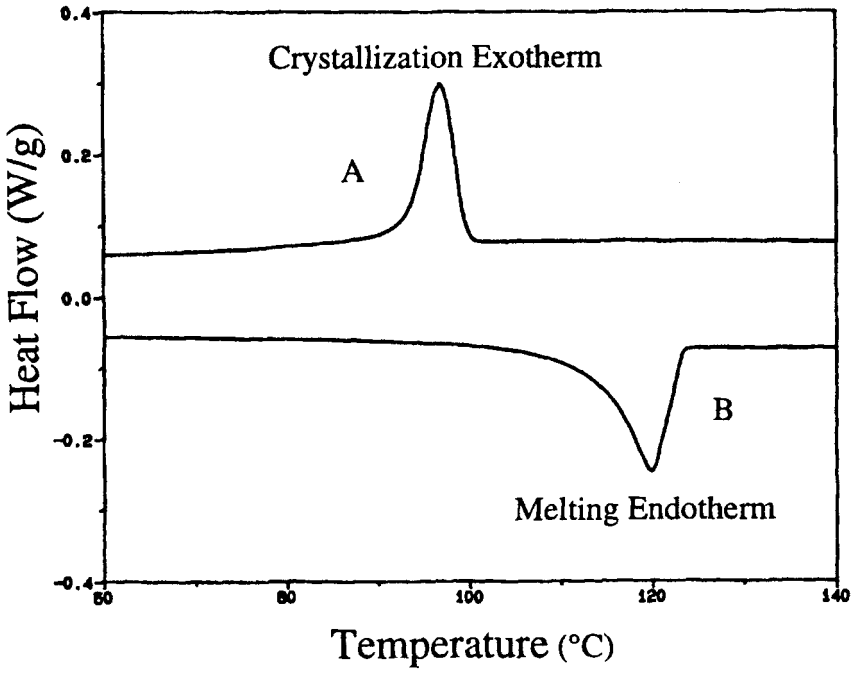

Figure 4. DSC plot for 12-methyl ester (**2a**): (A) cooling after first heating; (B) second heating.

X-Ray Diffraction

Powder X-ray diffraction patterns confirmed the calorimetric data. Sharp Bragg peaks in 12-*tert*-butyl ester (**1a**; Fig. 5, spectrum A) arose from scattering at well-defined crystalline regions in the unheated sample and became diffuse upon heating above the T_m (Fig. 5, spectrum B). In 12-methyl ester (**1b**), the presence of sharp Bragg peaks before and after heating above T_m confirmed recrystallization from the melt. Peak overlap in the powder diffraction pattern leading to ambiguous *I(hkl)* intensities inhibited complete structure resolution.[25]

DEA

The dielectric constant or permittivity (ε') measures the alignment of dipoles in an electric field and the loss factor (ε'') represents the energy required to align dipoles and move ions. Maxima in ε'' vs. temperature plots for *tert*-butyl esters (represented by dendrimer **2a** in Fig. 6) revealed a secondary, or β, relaxation process noted at low temperatures from 0.1 to 100,000 Hz, where frequency increased with temperature. The β transition in the *tert*-butyl esters was more pronounced than in the methyl esters, as shown by comparison of second generation dendrimers in Figure 7. The temperature of the transition increased with generation number; at 100 Hz, β transitions in tiers 1, 2, and 3 occurred at -84.3, -79.2, and -73.6°C, respectively. The observed broad peaks represent a spectrum of relaxation times. Peak maxima were assigned and the slope of the line obtained from Arrhenius plots (Fig. 8) of ln frequency vs. the reciprocal of temperature was used to calculate activation energies for the molecular motion encountered in the β process. This is similar to Arrhenius behavior that is commonly noted in linear polymers for secondary relaxation processes.[26] In the methyl esters, the peak maximum for each relaxation was less apparent; therefore, activation energies could not be calculated with certainty. It was observed that, in addition to secondary β relaxations, secondary γ relaxations were detected in the methyl ester dendrimers. Clear γ relaxations were observed in dendrimer **1b** between 6000 and 60,000 Hz; γ relaxations observed between 10 and 6000 Hz for dendrimer **3b** were less pronounced.

In broad terms, this Arrhenius behavior is characteristic of the movement of individual groups (e.g., such as individual ester and amide moieties) in macromolecules.[27] Figure 7 reveals stronger β relaxations in the *tert*-butyl esters than in methyl esters. This discrepancy in peak

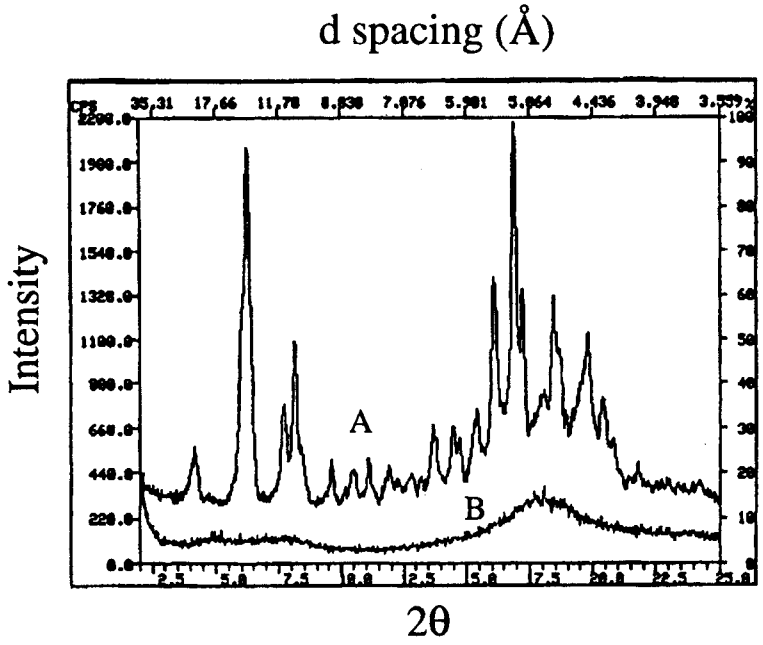

Figure 5. X-ray diffraction of 12- *tert*-butyl ester (**1a**): (A) before; and (B) after heating above T_m.

intensity may indicate that rotation of *tert*-butyl groups contributes to the β process. Expression of γ relaxations occurred only in the methyl esters and is thought to be partially attributed to dipolar amide groups.[28]

The complete nature of the β relaxation process cannot be identified with absolute certainty; however, two possible contributing mechanisms are suggested in separate studies conducted on macromolecules containing amide and *tert*-butyl ester

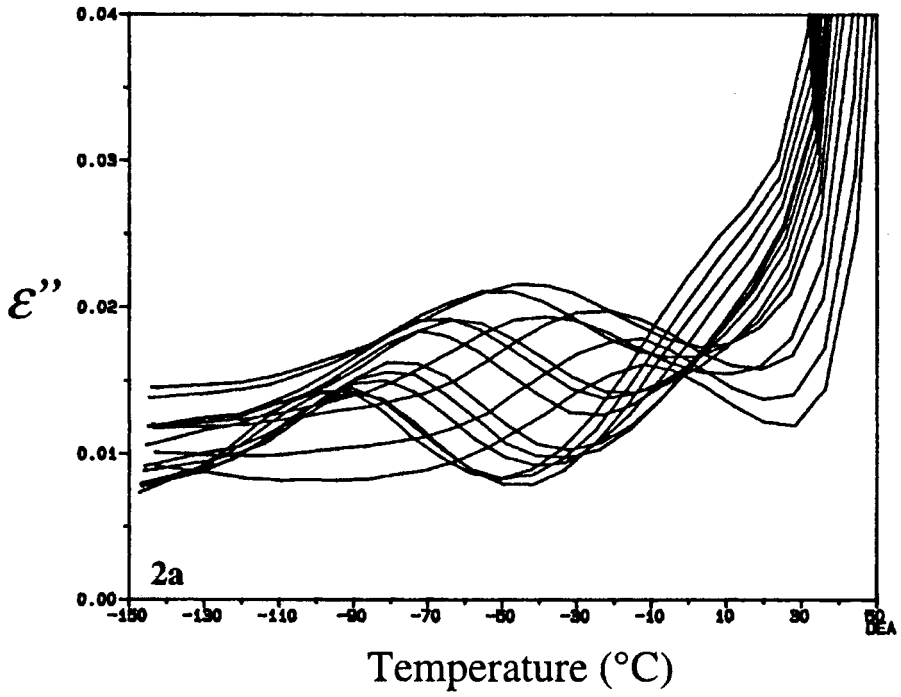

Figure 6. DEA plot for 36-*tert*-butyl ester (**2a**).

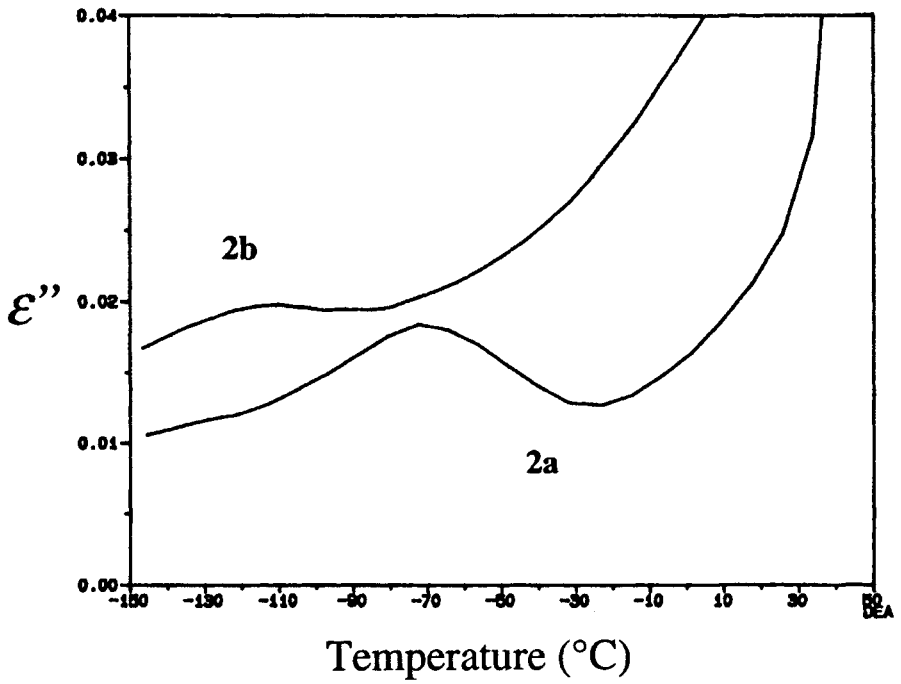

Figure 7. DEA plot in β relaxation region for 36-*tert*-butyl ester (**2a**) and 36-methyl ester (**2b**) at 300 Hz.

groups. Secondary β relaxations in polyamides (summarized by McCrum et al.[28]) were interpreted as the motions of dipolar (e.g., CH_2NH_2 and CH_2OH) chain end groups and the motions of chain segments including amide groups, which are not H-bonded to neighboring chains. The activation energy for the β process in these polymers was shown to vary between 13 and 21 kcal/mol.[29] A second possible mechanism could involve molecular motion of the bulky ester termini; hin-

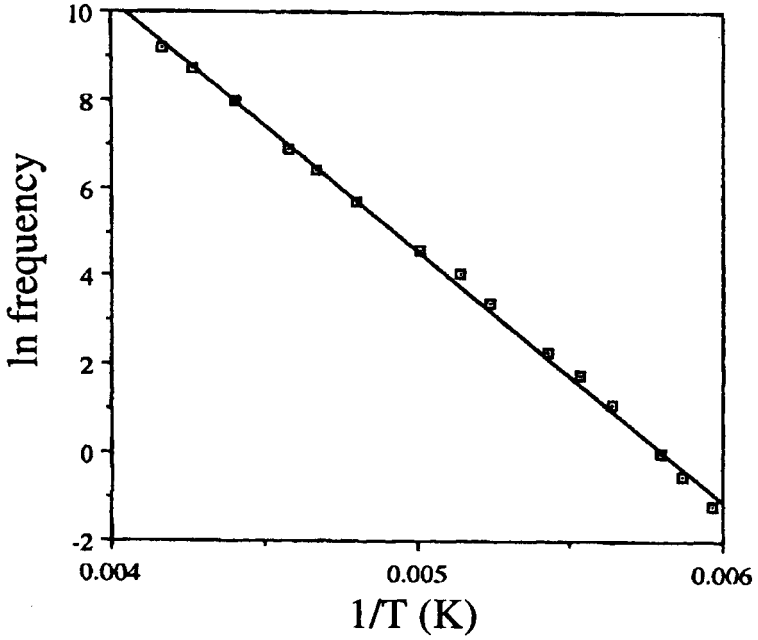

Figure 8. Arrhenius plot for β relaxation in 108-*tert*-butyl ester (**3a**).

Table IV. Activation Energies for β and γ Relaxations in kcal/mol

	1a	2a	3a	1b	2b	3b
β						
Scan 1	20.9	13.4	12.9	—	—	—
Scan 2	11.8	12.1	11.3	15.4	—	—
γ						
Scan 2				9.0	—	—

dered rotation of specific ester side-groups in poly(*tert*-butyl methacrylate) resulting in a 17 kcal/mol activation energy has been postulated.[30] Activation energies obtained in this study ranged between 11 and 21 kcal/mol. Both mechanical and dielectric data indicate that when the α and β transitions do not overlap, the activation energy for the β relaxation is independent of the size of the alkyl group.[29]

Table IV lists the calculated apparent activation energies for samples heated at 3°C/min. All β transitions observed in the amorphous dendrimers agreed within about ± 2 kcal/mol. However, it is noted that the crystalline dendrimer **1a** has a higher apparent activation energy in the first scan since molecular motion is impeded in the crystalline matrix requiring more thermal energy than in the "loose" amorphous matrix. As stated previously, the crystallinity in dendrimer **1a** was not recovered after a second heating; therefore, the apparent activation energy reported in the second scan is comparable to the values reported for the amorphous tiers **2a** and **3a**. Due to the inability to assign peak maxima for unclear relaxations in the methyl esters, all activation energies could not be calculated. The second scan for the first tier methyl ester (**1b**) resulted in an activation energy of 15.4 kcal/mol. This value for the crystalline matrix is less than the activation energy for the crystalline first tier of the *tert*-butyl ester (**1a**), 20.9 kcal/mol, indicating that motion associated with the β relaxation is more hindered in the *tert*-butyl-terminated dendrimer. The activation energy, 9.0 kcal/mol, for the γ relaxation observed in the methyl esters was obtained only for dendrimer **1b** and is comparable to values for γ relaxations noted in linear polymers.[28]

Both dipole polarization and ionic conduction contribute to dielectric spectra.[31,32] At temperatures at and below T_g, dielectric relaxations are encountered in which only the reorientation of dipoles is noted. At high temperatures and low frequencies, ionic conductance becomes significant.[23] In low frequency d.c. conduction, the hopping of mobile charge carriers is rapid over low free energy barriers in alignment with the electric field, while they accumulate when high free energy barriers are encountered. This results in a net polarization of the ionically charged system which contributes to ε' and ε''. At high frequencies, the periodic shift of the electric field prevents the accumulation of charges at high-energy barrier sites, thereby eliminating the net polarization discussed above.[33]

Conductive effects obscured the contribution of dipole alignment to ε'' in the dendrimers studied; thus, further treatment of the data was required. This marked dielectric loss at a temperature near T_g has been noted in amide-containing nylon polymers,[27,34] such as nylon-10,10 and the corresponding *N*-methylated derivatives, in which McCall and Anderson noted that, in the absence of an ionizable amide hydrogen, conductivity effects are minimized.[35] In order to observe the glass transition, the data were mathematically treated in terms of the electric modulus, M^*, which is defined as the inverse of complex permittivity, ε^*, where $\varepsilon^* = \varepsilon' - i\varepsilon''$ and $M^* = M' + iM''$[34] such that

$$M' + iM'' = (\varepsilon' - i\varepsilon'')^{-1} \quad (1)$$

$$M' = \frac{\varepsilon'}{(\varepsilon')^2 + (\varepsilon'')^2} \text{ and } M'' = \frac{\varepsilon''}{(\varepsilon')^2 + (\varepsilon'')^2} \quad (2)$$

Figure 9 depicts the dielectric loss function both before and after treatment with the electric modulus. M'' reveals the α relaxation, T_g, at approximately 80°C, as well as a second peak at 125°C. Starkweather and Avakian observed such a high temperature peak in dielectric studies on Nylon 6. They refer to this peak as a "conductivity relaxation" and note that it is due to algebraic properties of conductivity and does not reveal any information about the viscoelastic properties of the material.[34] Figure 10 shows the α transition at three frequencies.

The dendrimers exhibit classic polymeric dielectric behavior,[27] in which M'' absorptions (corresponding to the loss factor ε'') become broader and increase in height as the frequency increases. As observed for high polymers, a plot of ln frequency vs. the reciprocal of temperature for the glass-transition process is curved. It is well known that M″ curves can be shifted such that the

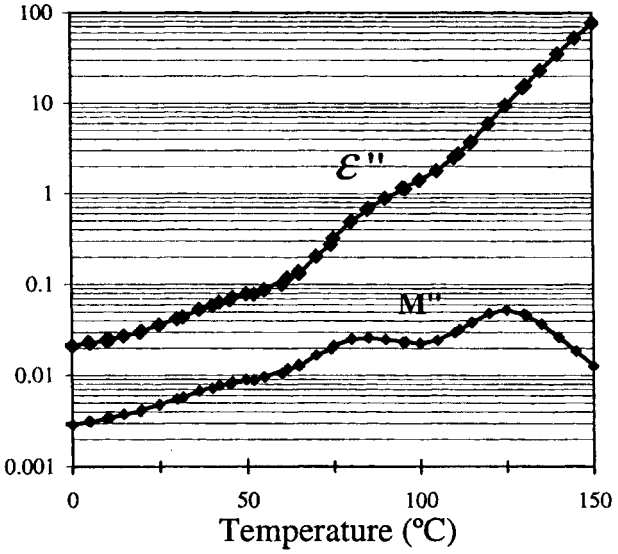

Figure 9. Dielectric loss function of 108-*tert*-butyl ester (**3a**).

maxima can be superimposed, and the shift factor (a_T) follows the WLF (Williams, Landel, and Ferry)[36] equation:

$$\ln a_T = \frac{-C_1(T - T_o)}{C_2 + (T - T_o)} \tag{3}$$

where a_T corresponds to frequency, C_1 and C_2 are WLF constants, T is a given temperature, and T_o is the reference temperature which corresponds to T_g.

The values C_1, C_2, and T_o were determined by curve fitting the data to the WLF equation (Fig. 11). Activation energies were calculated according to the method of Catsiff and Tobolsky[37]:

$$\Delta H = 2.303(C_1/C_2)RT_g^2 \tag{4}$$

The WLF constants C_1 and C_2 provide information regarding the fractional free volume in the glass transition region (f_g) and the thermal expansion coefficient (α_f)[36] as illustrated in the following equations:

$$f_g = B/(2.303 \times C_1) \tag{5}$$

$$\alpha_f = f_g/C_2 \tag{6}$$

where f_g is defined as the unoccupied (free) volume in the structure and B is taken as unity, according to Doolittle.[38] Data, obtained in the glass-transition region, are shown in Table V. As T_g increased, the apparent activation energy drastically increased since T_g involves large-scale motion. As the generation number increased, branching and the number of chain ends also increased; thus, f_g became larger in the *tert*-butyl esters, as did α_f. The methyl esters, however, exhibited the opposing trend indicating more effective packing with increasing generation number. Trends in the calculated thermal expansion coefficients matched those for free volume as a function of tier number.

As the molecular weight and branching of the structure increase, molecular motion becomes more complex. Therefore, although not shown, a broadening of ε'' peaks was observed with increasing generation number that reflected an increase

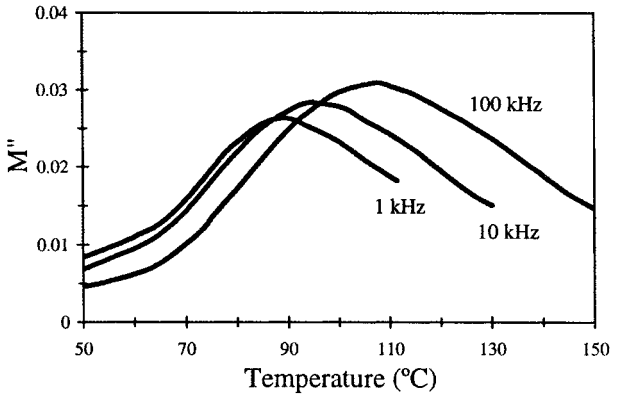

Figure 10. Frequency dependence of glass transition for 108-*tert*-butyl ester (**3a**) after treatment with the electric modulus.

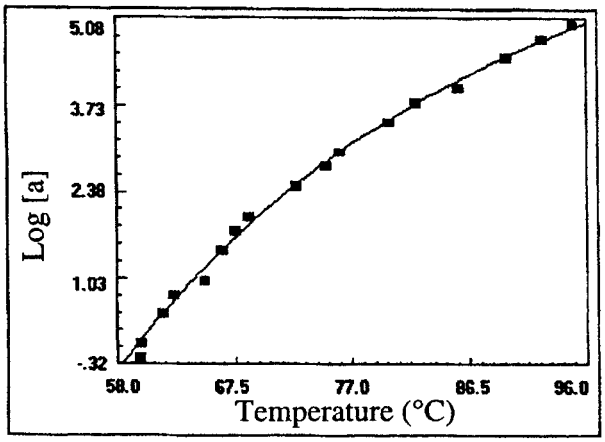

Figure 11. WLF plot for glass transition of 36-*tert*-butyl ester (**2a**).

Table V. Data Obtained for α Relaxations

	1a	2a	3a	1b	2b	3b
ΔH (kcal/mol)	99.1	125.6	167.9	79.3	102.9	99.4
T_g (°C)	44.3	59.6	75.6	15.7	40.4	53.3
C_1	16.5	11.4	10.8	10.6	11.6	13.9
C_2	76.8	46.0	35.8	50.9	50.6	68.2
f_g	0.0263	0.0381	0.0402	0.0410	0.0375	0.0312
α_f (10^{-3})	0.342	0.828	1.12	0.806	0.741	0.457

in the spectrum of relaxation times. The magnitude of the activation energy and fit to the WLF equation in the glass transition of dendrimers are also characteristic of long-chain polymers. Values for the constants C_1 and C_2, however, do vary from the "universal" constants reported[36,39] for high polymers (C_1 = 17.4 and C_2 = 51.6).[36,39] In linear polymers, the glass transition has been largely attributed to translational motion of entire molecules and cooperative motion of chain segments approximately 40–50 carbon atoms in length.[40] When considering the differing structure of dendritic macromolecules, it is very interesting to note that even the lowest molecular weight dendrimer conforms to WLF behavior. This finding points to the need to redefine molecular motion throughout the glass-transition region in linear polymers.

The dielectric data were further analyzed in the β transition region via the Cole–Cole method[28,41] where ε'' was plotted against ε' for a series of frequencies at a constant temperature; data acquisition was repeated in 5°C increments. Plots deviated from semicircular behavior, indicating that a spectrum of relaxation times is associated with the β process. Figure 12 is a representative Cole–Cole plot for the β process. Intersection with the x-axis occurs at two points (ε_∞, representing the high frequency, unrelaxed state followed by ε_o, representing the low frequency, relaxed state). The difference between these states, $\Delta\varepsilon$, yielded dielectric (relaxation) strengths. Table VI lists $\Delta\varepsilon$ values for β relaxations, which were found to increase with generation number. Dielectric strengths for β relaxations were obtained only for *tert*-butyl esters, since Cole–Cole plots for methyl esters were unclear. Values for $\Delta\varepsilon$ for β relaxations were comparable to those obtained for amorphous linear polymers studied in our laboratory.[42]

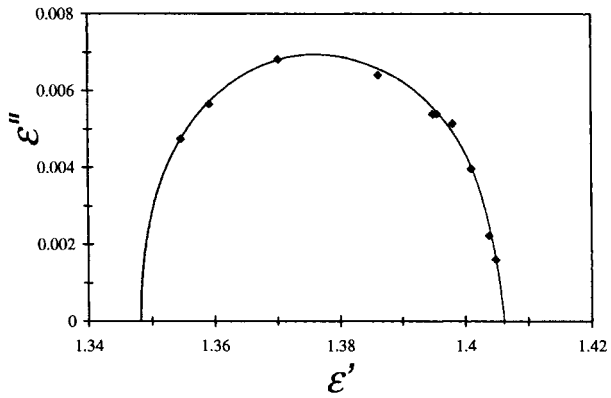

Figure 12. Cole–Cole plot for β relaxation in 12-*tert*-butyl ester (**1a**) at −140°C.

The electric modulus approach was also extended to the Cole–Cole method for α[34,43,44] and β[44] relaxations to give $\Delta M'$. Representative Cole–Cole plots of M'' vs. M' are depicted in Figure 13 in which complex behavior was observed for the α process. Contrary to traditional Cole–Cole plots (ε'' vs. ε'),[41] M' values proceed from lower to higher frequencies; thus, the left-hand intersection of the curve with M' represents the relaxed state (M_o) while the right-hand intersection represents the unrelaxed state (M_∞). Greater values were characteristic of the large-scale motion associated with α (glass) transitions, while the small-scale motion encountered in the β process produced strengths of a lesser magnitude. Relaxation strengths, which were comparable for *tert*-butyl and methyl ester structures in the glass-transition region, were found to increase with generation number. Relaxations in complex dielectric plots were obscured in the β region for the methyl esters, as well as in the α region of the incomplete third tiers for both families.

Cole–Cole representations of high temperature, conductivity relaxations revealed semicircular behavior with the low frequency end intersecting the origin of the M' axis. This behavior corresponds closely to a Debye single-relaxation

Table VI. Dielectric Strengths

	1a	2a	3a	1b	2b	3b
$\Delta\varepsilon$						
β	0.0688	0.161	0.248	—	—	—
ΔM						
β	0.0338	0.0394	0.0435	—	—	—
α	0.113	0.244	—	0.112	0.251	—

process as was noted by Starkweather et al. for Nylon 6.[34]

The ionic conductivity, σ, is given in the following equation[23,34]:

$$\sigma = \varepsilon'' \omega \varepsilon_o \tag{7}$$

where ω is the angular frequency ($2\pi f$) and ε_o is the absolute permitivitty of free space (8.85×10^{-12} F/m). Figure 14 depicts plots of log conductivity (pmho/cm) vs. absolute temperature (1000/T(K)) for the first tiers of (**1a**) *tert*-butyl and (**1b**) methyl esters. Dendrimers **1a**, **2a**, **3a**, **2b**, and **3b** exhibited Arrhenius behavior at temperatures greater than T_g where ionic conductivity was prevalent; apparent activation energies obtained were 9.1, 10.4, 9.5, 8.7, and 9.4 kal/mol, respectively. Starkweather and Avakian[34] also observed this linear relationship for conductivity in nylons 6, 66, and 6I obtaining apparent activation energies that ranged from 24 to 44 kcal/mol. They concluded that movement of polymer segments is necessary for the migration of charged species. Arrhenius behavior was not obeyed by dendrimer **1b** as seen by the discontinuity observed at approximately 2.7 K^{-1}; this value corresponds to 97°C which is the temperature at which recrystallization from the melt occurs.

CONCLUSIONS

In summary, both the chemical nature (functionality) and branching complexity of the molecular structures influenced the ability of these macromolecules to assemble into crystalline lattices. First generation *tert*-butyl ester was crystalline only upon recovery from solution, whereas crystallinity in the first generation methyl ester was also recovered from the melt. *Tert*-butyl esters exhibited clear β relaxations that increased in temperature with generation number. Secondary relaxations in methyl esters were less pronounced, however, apparent activation energies for the β and γ process in the first tier were determined. Secondary relaxations were characterized by Arrhenius behavior and their apparent activation energies were calculated accordingly.

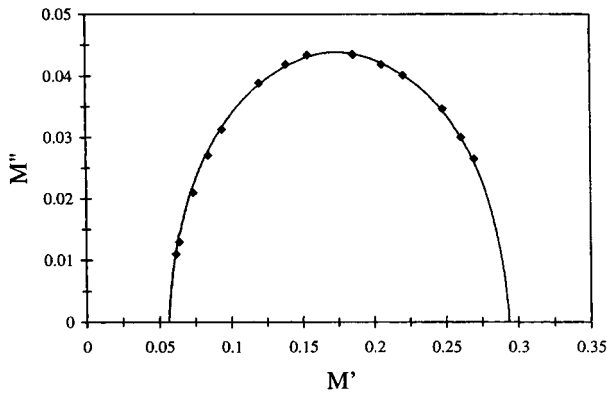

Figure 13. Cole–Cole representation for α relaxation in 36-methyl ester (**2b**) at 65°C.

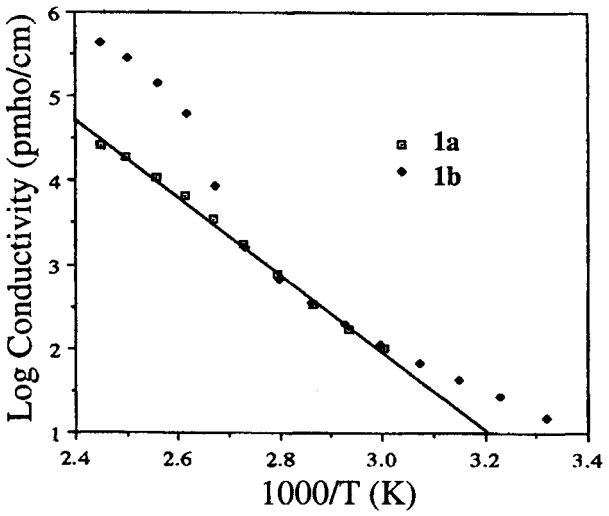

Figure 14. Conductivity in 12-*tert*-butyl ester (**1a**) and 12-methyl ester (**1b**).

When ionic conductivity effects were removed through mathematical treatment with the electric modulus, the glass transition was revealed. *Tert*-butyl and methyl esters exhibited well-defined glass (α) transitions whose temperatures increased with generation number. Adherence to WLF behavior allowed determination of apparent activation energies, as well as, calculation of free volume (f_g) and thermal expansion coefficients (α_f) which are related to the WLF constant C_1 and C_2, respectively. Values for f_g and α_f increased with generation number in *tert*-butyl esters. The methyl esters, however, exhibited the opposing trend indicating more effective packing with increasing tiers. Apparent activation energies in the glass-transition region also increased with generation number. Relaxation strengths also increased with generation number; values were comparable for *tert*-butyl and methyl ester structures in the glass-transition region. Electric modulus data also revealed conductivity relaxations, at temperatures above the glass transitions, which conform to the Debye process for a single relaxation time. The physical characterization of the above relaxations is significant as it provides insight into molecular motion in dendrimers.

This work (GRN) was supported by the National Science Foundation (DMR-96-22609). We also gratefully acknowledge Dr. Gregory Baker for his expertise in MALDI-TOF MS, Dr. Katherine Williams (University of Florida) for providing access to TGA instrumentation, and Dr. David Mallinson (USF, Department of Marine Sciences) for aid in X-ray diffraction instrumentation. We would also like to thank Dr. Charles Moorefield and Enfie He for their contributions.

REFERENCES AND NOTES

1. Newkome, G. R.; Yao, Z.; Baker, G. R.; Gupta, V. K. J Org Chem 1985, 50, 2004.
2. Tomalia, D. A.; Baker, H.; Dewald, J. R.; Hall, M.; Kallos, G.; Martin, S.; Roeck, J.; Ryder, J.; Smith, P. Polym J 1985, 17, 117.
3. Voit, B. I. Acta Polym 1995, 46, 87.
4. Wooley, K. L; Hawker, C. J.; Pochan, J. M.; Fréchet, J. M. J. Macromolecules 1993, 26, 1514.
5. de Brabander-van den Berg, E. M.; Meijer, E. W. Angew Chem, Int Ed Engl 1993, 32, 1308.
6. Stutz, H. J. J Polym Sci Part B: Polym Phys 1995, 33, 333.
7. Turner, S. R.; Voit, B. I.; Mourey, T. H. Macromolecules 1993, 26, 4617.
8. Turner, S. R.; Walter, F.; Voit, B. I.; Mourey, T. H. Macromolecules 1994, 27, 1611.
9. Kim, Y. H.; Beckerbauer, R. Macromolecules 1994, 27, 1968.
10. Newkome, G. R.; Moorefield, C. N.; Vögtle, F. Dendritic Molecules—Concepts, Syntheses, Perspectives; VCH Verlag: Weinheim, Germany, 1996.; Moorefield, C. N.; Newkome, G. R. in G. R. Newkome, Ed., Advances in Dendritic Macromolecules; JAI Press: London, 1994; Vol. 1, p. 58.; Fréchet, J. M. J. Science 1994, 263, 1710; Ardoin, N.; Astruc, D. Bull Soc Chim Fr 1996, 132, 875.
11. Percec, V.; Chu, P.; Ungar, G.; Zhou, J. J Am Chem Soc 1995, 117, 11441.
12. Mourey, T. H.; Turner, S. R.; Rubenstein, M.; Fréchet, J. M. J.; Hawker, C. J.; Wooley, K. L. Macromolecules 1992, 25, 2401.
13. DeGennes, P. G.; Hervert, H. J. J Phys Lett 1983, 44, L-351.
14. Hawker, C. J.; Farrington, P. J.; Mackay, M. E.; Wooley, K. L.; Fréchet, J. M. J. J Am Chem Soc 1995, 117, 4409.
15. Kim, Y. H.; Webster, O. W. Macromolecules 1992, 25, 5561.
16. Massa, D. J.; Shriner, K. A.; Turner, S. R.; Voit, B. L. Macromolecules 1995, 28, 3214.
17. Malmström, E.; Liu, F.; Boyd, R. H.; Hult, A.; Gedde, U. W. Polym Bull 1995, 32, 679.
18. Hult, A.; Malmström, E.; Johansson, M. Polym Mater, Sci Eng 1995, 73, 173.
19. Malmström, E.; Hult, A.; Gedde, U. W.; Liu, F.; Boyd, R. H. Polymer 1997, 38, 4873.
20. Young, J. K.; Baker, G. R.; Newkome, G. R. Macromolecules 1994, 27, 3464.
21. TGA 2950 Thermogravimetric Analyzer, TA-031, TA Instruments.
22. DSC 2920 Differential Scanning Calorimetry, TA-087A, TA Instruments.
23. DEA 2970 Dielectric Analyzer, TA-057, TA Instruments.
24. Miller, T. M.; Kwock, E. W.; Neenan, T. X. Macromolecules 1992, 25, 3143.
25. Harris, K. D. M.; Tremayne, M. Chem Mater 1996, 8, 2554.
26. Gedde, U. W. Polymer Physics; Chapman and Hall: London, 1995.
27. Gao, H.; Harmon, J. Thermochim Acta 1996, 284, 85.
28. McCrum, N. G.; Read, B. E.; Williams, G. Anelastic and Dielectric Effects in Polymeric Solids; Dover: New York, 1991.
29. Starkweather, Jr., H. W.; Barkley, J. R. J Polym Sci: Polym Phys Ed 1981, 19, 1211.
30. Mikhailov, G. P. Physics of Non-Crystalline Solids; North Holland: Amsterdam, 1965, p. 270.
31. Parthun, M. G.; Johari, G. P. J Chem Soc Faraday Trans 1995, 91, 329.
32. Johari, G. P.; Pathmanathan, K. Phys Chem Glasses 1988, 29, 219.

33. Macedo, P. B.; Moynihan, C. T.; Bose, R. Phys Chem Glasses 1972, 13, 171.
34. Starkweather, H. W.; Avakian, P. J Polym Sci Part B: Polym Phys 1992, 30, 637.
35. McCall, D. W.; Anderson, E. W. J Chem Phys 1960, 32, 237.
36. Aklonis, J.; MacKnight, W.; Shen, M. Introduction to Polymer Viscoelasticity; Wiley-Interscience: New York, 1972.
37. Catsiff, E.; Tobolsky, A. V. J Colloid Sci 1955, 10, 375.
38. Doolittle, A. K. J Appl Phys 1951, 22, 1471; 1952, 23, 236.
39. Freid, J. R. Polymer Science and Technology; Prentice-Hall PTR: NJ, 1995.
40. Rosen, S. R. Fundamental Principles of Polymeric Materials; John Wiley & Sons: New York, 1993.
41. Havriliak, Jr., S.; Havriliak, S. J. Dielectric and Mechanical Relaxation in Materials: Analysis, Interpretation, and Application to Polymers; Hanser Publications: Munich, 1997.
42. Bertolucci, P.; Harmon, J. *in* S. Jenekje and K. Wynne, Eds., Photonic and Optoelectronic Polymers; American Chemical Society: Washington, D.C., 1997; pp. 79–97.
43. Calleja, R. D. J Non-Cryst Solids 1994, 172–174, 1413–1418.
44. Calleja, R. D.; Matveeva, E. S.; Parkhutik, V. P. J Non-Cryst Solids 1995, 180, 260.